Supplemental Information

Device fabrication

For the weave and coil chip designs, SU8 2025 (MicroChem Corp., MA) was spun at 3500 rpm to a thickness of 20µm, soft baked at 65°C, 95°C and 65°C for 2, 4, and 2 minutes, respectively, followed by a 5s exposure at 42.5mW/cm^2. The post exposure bake was identical to the soft bake. Unexposed resist was removed during a 2min immersion development step. Features in the thick PDMS layer of the sample chip used for channel writing were cast on 50µm high SU8-50 features. The photoresist was spun at 2000rpm, soft baked at 65°C, 95°C and 65°C for 6, 20, and 6 minutes, respectively, followed by a 7s exposure. The post exposure bake was carried out at the same temperatures at the soft bake for 2, 8, and 2 minutes, respectively. The thin PDMS layer of the multi-laminate stream mixer was cast from a hybrid mould consisting of 10µm high SU8-5 features and SU8-2025. SU8-5 was spun at 1500rpm, soft baked at 65°C, 95°C and 65°C for 2, 5, and 2 minutes, respectively, and exposed for 5s. The post exposure bake was carried out at 65°C, 95°C and 65°C for 1, 3, and 1 minutes, respectively. SU8-5 features were developed for 1min. The thick PDMS layer was cast on SU8-100 which was spun to a thickness of 100µm at 3000rpm, soft baked at 65°C, 95°C and 65°C for 10, 45, and 10 minutes, respectively. The exposure for 12s was followed by a post exposure bake step at 65°C, 95°C and 65°C for 2, 12, and 1 minutes, respectively. The development was complete after 7min.

Microfluidic devices were fabricated by Multilayer Soft Lithography (MSL) as described elsewhere.[1] Briefly, moulds were exposed to trichloromethylsilane vapour (Alfa Aesar, MA) for 30min. PDMS prepolymer RTV 615 (General Electrics, NY) was mixed at a ratio of 5:1 (A:B) and 20:1 for the thick and the thin PDMS layers, respectively. Bubbles in the uncured PDMS were removed by degassing the 5:1 mixture in a vacuum chamber for 1h. The uncured 20:1 PDMS was spun at 2000rpm. Each layer was partly cured at 80°C for 45min. Following layer alignment, layers bonded covalently to each other after 45min at 80°C.

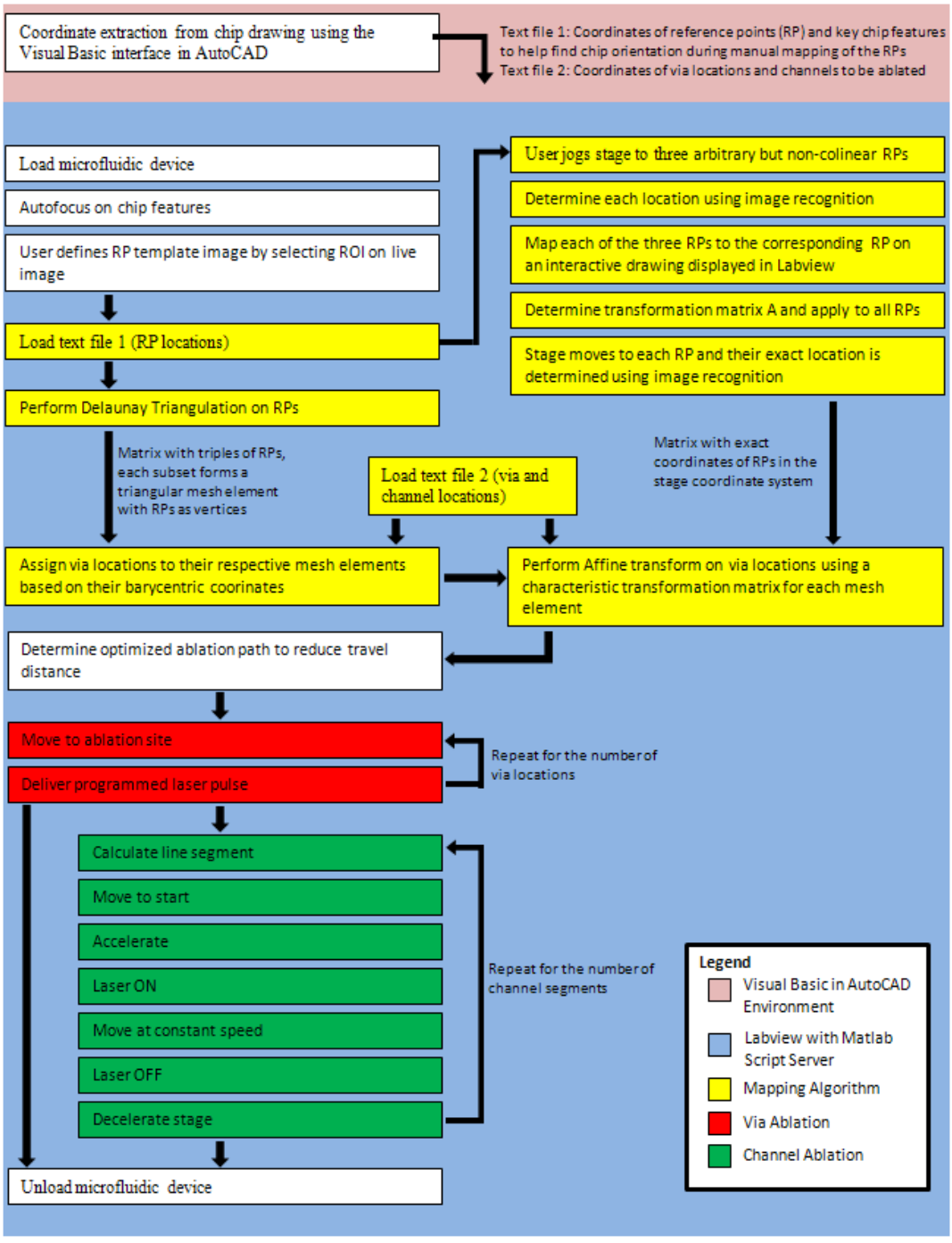

Fig. S1 Flow chart of the ablation process: TXT files containing the coordinates of reference points and via locations are generated using a Visual Basic script in AutoCAD. Following an autofocus step, these files are loaded in LabView. A mesh is generated using reference points as vertices and via locations are determined using Affine Transform (see text for details). A laser pulse with a predetermined pulse width is delivered to each ablation site. Optionally, straight channel segments can be ablated following the ablation of interlayer connections.

Local deformation correction

Mesh generation by Delaunay Triangulation

A mesh consisting of M mesh elements is generated using Delaunay Triangulation where the reference points coincide with the vertex points. In this triangulation method, the circumcircle of each mesh element does not enclose any other vertex points.[2] Delaunay Triangulation maximizes the minimum angle in each mesh element thereby avoiding skinny triangles. As a consequence, triangles are more compact and represent the local chip deformation more adequately than mesh elements consisting of vertices that are spaced further apart.

Via assignment using barycentric coordinates

After generating a mesh, via locations are assigned to their respective mesh element: barycentric coordinates[3] of the nth via location r_n are computed with respect to a mesh element m as

$$\vec{r}_n = \lambda_{m,1}\vec{v}_{m,1} + \lambda_{m,2}\vec{v}_{m,2} + \lambda_{m,3}\vec{v}_{m,3} \qquad \text{(S1)}$$

where $r_n=(r_{n,x},r_{n,y})$ denotes the nth via location, $v_{m,i}=(v_{m,i,x}, v_{m,i.y})$ the vertex points (reference points) of the triangle T_m and $\lambda_{m,i}$ the barycentric coordinates with respect to T_m. Any point r located on the triangle T_m may be expressed as a weighted sum of the three vertices with the constraint $\lambda_{m,1}+\lambda_{m,2}+\lambda_{m,3}=1$. It follows that via locations are assigned to the mesh element for which $0 \le \lambda_{m,i} \le 1 \forall i$ holds. If a via location cannot be assigned to any of the mesh elements, i.e. it is outside the generated mesh, it is assigned to the closest triangle centroid. Using the constraint given above, S1 can also be expressed with matrices as

$$\vec{r}_n - \vec{v}_{m,3} = T \cdot \lambda_m \quad \text{where} \quad T = \begin{bmatrix} (v_{m,1,x} - v_{m,3,x}) & (v_{m,2,x} - v_{m,3,x}) \\ (v_{m,1,y} - v_{m,3,y}) & (v_{m,2,y} - v_{m,3,y}) \end{bmatrix} \qquad \text{(S2)}$$

The barycentric coordinates can therefore be determined by solving equation S2 for λ_m.

Linear transformation

Affine transform[4] is used twice during the mapping process: it is first employed to determine the approximate location of reference points. Once these have been detected, affine transform is applied to each individual mesh element.

The algorithm for determining the exact via locations on a microfluidic device is as follows: prior to ablation, the operator manually jogs the stage to sequentially bring three arbitrary but non-collinear reference points into view. The exact position of the three reference points are determined by image recognition. From these three reference points the remaining reference points are roughly mapped to the stage coordinate system by solving for the affine transformation matrix A_{sys} as

$$\begin{pmatrix} x_i' \\ y_i' \\ 1 \end{pmatrix} = \begin{pmatrix} a_{11} & a_{12} & a_{13} \\ a_{21} & a_{22} & a_{23} \\ 0 & 0 & 1 \end{pmatrix} \begin{pmatrix} x_i \\ y_i \\ 1 \end{pmatrix} \qquad \text{(S3)}$$

where (x_i,y_i) and (x_i',y_i') represent the reference point coordinates on the drawing and on the microfluidic device, respectively. Three coordinate sets are required to solve for the transformation matrix A_{sys} with six unknowns.

The stage subsequently moves to the estimated position of each reference point to exactly locate its coordinates using image recognition. Once all reference points are located, a unique transformation matrix A_m is calculated for each triangle T_m. A_m is applied to all via locations that are circumscribed by the triangle T_m as previously determined using barycentric coordinates. Since reference points can be arbitrarily positioned, this method allows for a high degree of design flexibility.

Multi-laminate Mixer

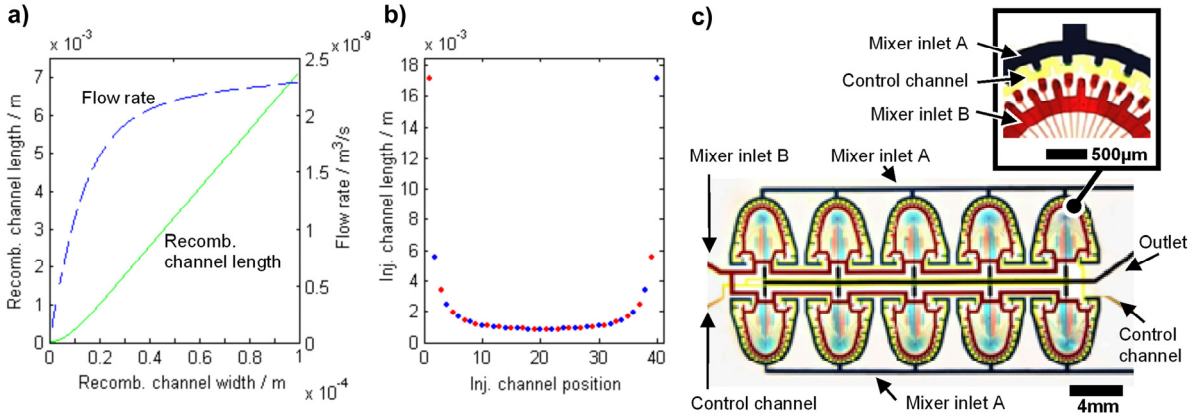

Fig. S2 (a) Depending on the chosen width of the recombination channel, the length needs to be adjusted so that mixing can go to completion before the two reagents exit the recombination channel. The width and the length of the recombination channel determine the flow rate at a given pressure (276 kPa, 40 psi). (b) Evenly spaced flow streams require different flow rates through the injection channels and necessitate the adjustment of the injection channel length. (c) Micrographs of the multi-laminate stream mixer. An array of 10 mixer elements allows for flow rates of up to 1 mL/min. (Inset) Prior to mixing, all control channels are actuated allowing for outgas priming of the flow channels.

Injection channels

If the flow rate through each of the injection channels was identical, this would result in streamlines with different widths due to the flow profile in the recombination channel and no-slip boundary conditions at the channel walls. Since the linear flow velocity is zero at the channel walls and increases towards the centre of the channel, streamlines closer to the channel walls would be considerably wider. As the time for mixing of two given reagents depends on the diffusion length across the streamlines, mixing can be enhanced by adjusting the flow rates through each of the inlet channels resulting in equally spaced streamlines. The required flow rates through each of the inlet channels, however, depend on the dimensions of the recombination channel (Figure S2). The velocity profile in the recombination channel is given by

$$v_x(y,z) = \frac{4h_r^2 \Delta p}{\pi^3 \eta s_r} \sum_{n,odd}^{\infty} \frac{1}{n^3} \left[1 - \frac{\cosh\left(n\pi \, y/h_r \right)}{\cosh\left(n\pi \, w_r/2h_r \right)} \right] \sin\left(n\pi \, z/h_r \right) \qquad \text{(S4)}$$

where h_r, s_r, Δp, η are the height and length of the recombination channel, the pressure drop and the viscosity, respectively. The parameters y and z are considered within the intervals $-w_r/2 \le y \le w_r/2$ and $0 \le z \le h_r$, respectively. The desired flow rate of each streamline is therefore

$$Q_{st,i} = \int_0^{h_r} \int_{y_{1,i}}^{y_{2,i}} v_x(y,z)\, dy dz$$

$$Q_{st,i} = \frac{h_r^3 w_r \Delta p}{12 \eta s_r} \left[1 - \sum_{n,odd}^{\infty} \frac{1}{n^5} \frac{192}{\pi^5} \frac{h_r}{w_r} \tanh\left(n\pi \frac{w_r}{2h_r} \right) \right] \qquad \text{(S5)}$$

Compared to the streamlines in the channel centre, lower flow rates are required for streamlines closer to the channel walls. Since the relative resistance of each injection channels r_i compared to the one with the lowest resistance is anti-proportional to the relative flow rates q_i in the streamlines, r_i can be expressed as

$$r_i = \frac{1}{q_i} = \frac{Q_{st,\max}}{Q_{st,i}} = \frac{R_{inj}}{R_{inj,\min}} \qquad \text{(S6)}$$

where $Q_{st,max}$ and $Q_{st,I}$ are the maximum flow rate and the flow rate through each of the injection channels, respectively. R_{inj} and $R_{inj,min}$ are the impedance of each injection channel and the minimum impedance, respectively. Since $Q = \Delta p / R$, the length of the injection channel can be determined numerically using Equation (S5). Generally, the resistance of the injections channels can be tuned by adjusting the width, the length or a combination thereof. While adjusting the width would allow for a more compact mixer design, it is typically more challenging to precisely

control the width in photolithographic processes. This prompted us to vary the length of the injection channel as a means of controlling the relative flow rates (Figure S2b).

Recombination channel

Since the recombination channel can substantially increase the flow impedance, its dimensions also influence the throughput of the mixer: while a narrow channel would reduce the diffusion length across the streamlines and would therefore result in a shorter mixing time, it also causes the flow resistance to increase. On the other hand, a wider channel results in a longer diffusion time and requires a longer channel so that the mixing goes to completion before the outlet of the mixer is reached. A longer channel in turn increases the overall resistance. Dimensional parameters therefore need to be balanced carefully while the ease of fabrication should be considered.
The total flow rate Q_r through the recombination channel is given by

$$Q_r = A_r \cdot v_r = w_r h_r \cdot \frac{s_r}{t} \tag{S7}$$

where A_r, v_r, w_r, h_r, s_r are the cross-section area of the recombination channel, the linear flow velocity, the width, height and length, respectively. The time t that the fluid needs to spend in the recombination channel should be equal to or greater than the diffusion time that is required to diffuse across adjacent streamlines:

$$t \geq \frac{w_{st}^2}{2D} = \frac{(w_r/N)^2}{2D} \tag{S8}$$

where w_{st}, D, and N are the width of the streamlines, the diffusion coefficient, and the number of alternating streamlines in the recombination channel. Combining Equations (S5),(S7), and (S8), this results in a required length of the recombination channel of

$$s_r = \frac{w_r h_r}{N} \sqrt{\frac{\Delta p}{24 \eta D}\left[1 - \sum_{n,odd}^{\infty} \frac{1}{n^5} \frac{192}{\pi^5} \frac{h_r}{w_r} \tanh\left(n\pi \frac{w_r}{2h_r}\right)\right]} \tag{S9}$$

Recognizing that the flow resistance of the recombination channel dominates the system, the mixer was designed for a pressure drop of 276 kPa (40 psi) across the recombination channel to maximize the throughput (Figure S2a). In this case, the overall pressure drop does not exceed 414k Pa (60 psi) above of which delamination of a multilayer PDMS device may occur.

Since the multi-laminate stream mixer requires the fabrication of valves with a feature height of 20 µm, the same resist was used for the recombination channel for the ease of fabrication. The number of injection channels N is limited by the feature resolution of the masks used for the photolithographic process. In particular, the achievable feature density at the intersection of the injection channels imposes constraints on the number of injection channels. In addition, the aspect ratio of features in the joining region is to be considered to avoid channel collapsing at the intersection. An injection channel width of 10 µm at the intersection results in an optimal number of injection channels of N = 40.

Total expenses

Table S1 Approximate costs of the ablation system

Cost (US$)	**Item**
6000	CO2 Laser
2410	IR beam forming and delivery optics (3 mirrors, 3 lenses, 1 beam combiner)
300	Optical mounts
2200	Imaging system (in-line tube, CCD, fibre light)
150	Frame grabber
1200	National Instruments DIO Card, connector boards, cables
530	Motors, drivers and sensors for loading stage
530	Motors, drivers and sensors for autofocus system
4000-20000	xy-stage, drivers, controller (depending on accuracy and speed of the stage)
600	Custom mounts, panels, safety enclosures
180	AutoCAD
2600	Labview Full Development System
20700-36700	**Total**

References

1. M. A. Unger, H. P. Chou, T. Thorsen, A. Scherer and S. R. Quake, *Science*, 2000, **288**, 113-116.
2. M. De Berg, O. Cheong, M. Van Kreveld and M. Overmars, *Computational geometry: algorithms and applications*, Springer-Verlag New York Inc, 3rd ed., 2008, pp. 191-218.
3. J. A. Vince, *Mathematics for computer graphics*, Springer Verlag, 2nd ed., 2006, pp. 193-221.
4. J. D. Foley, A. Van Dam, S. K. Feiner and J. F. Hughes *Computer graphics: principles and practice*, Addison-Wesley, 2nd ed., 1995, pp. 201-226.